Effect of shoulder geometry on residual stress and fatigue properties of AA6082 fsw joints [†]

M. De Giorgi[1,*], A. Scialpi[2], F.W. Panella[1] and L.A.C. De Filippis[2]

[1]*Dipartimento di Ingegneria dell'Innovazione, Università degli Studi del Salento, Lecce, Italy*
[2]*Dipartimento di Ingegneria dell'Ambiente e per lo Sviluppo Sostenibile, Politecnico di Bari, Taranto, Italy*

Abstract

The tool geometry is a crucial characteristic of the friction stir welding (FSW) process; its design is the key to the successful FSW application for a wide range of materials and thicknesses improving the weld strength and fatigue life. The present study investigates the influence of three shoulder geometries on the FSW joint performance, in terms of residual stresses state, microhardness profile and mechanical properties of 1.5 mm thick AA 6082-T6 FSW joints in the butt-joint configuration. The three tool geometries are characterized by three different shoulders: a shoulder with scroll, a shoulder with a shallow cavity, and a flat shoulder. Transverse and longitudinal tensile tests at room temperature were performed in order to evaluate the mechanical properties, respectively, of the joints and of the stirred zone, while the fatigue tests were performed transversally to the joint line.

Keywords: AA6082T6; Fatigue; Friction Stir Welding; Shoulder geometry; Residual stresses

1. Introduction

Al-Mg-Si alloys (6xxx series) are widely used as-medium-strength structural alloys, which have the additional advantages of good formability, corrosion resistance, immunity to stress corrosion cracking, and low cost [1-3]. Different from high strength aluminium alloys (2xxx and 7xxx series), 6xxx alloys can be welded by traditional fusion welding techniques like tungsten inert gas (TIG) and metal inert gas (MIG). Nevertheless, friction stir welding (FSW) joints are usually stronger [4-6] and less expensive [7] than fusion welds. This is why FSW is attracting an increasing amount of interest in automotive and shipbuilding industries where 6xxx alloys are extensively used.

FSW is a new solid state welding method devel-

[†] This paper was recommended for publication in revised form by Associate Editor Jooho Choi
[*]Corresponding author. Tel.: +39 832 297776, Fax.: +39 832 297768
E-mail address: marta.degiorgi@unile.it
© KSME & Springer 2009

---

oped and patented by Thomas et al. in 1991 [8]. This welding process is well suited for joining aluminium alloys, especially the high strength alloys, which are considered unweldable by conventional fusion welding techniques, because it avoids the dentritic structure formed in the fusion zone which can seriously reduce the mechanical properties of the joint [9, 10].

FSW is a continuous solid-state welding process involving a non-consumable rotating tool, which consists of a probe with a concentric larger diameter shoulder (Fig. 1). The material being joined is rapidly friction heated, by tool rotation, to a temperature at which it is easily plasticized. The yield strength of the metal, at the interface between the rotating tool and the workpiece, falls below the applied shear stress, as the temperature rises so that the plasticized material is extruded from the leading side to the trailing side of the tool. The tool is then steadily moved along the joint line with the plasticized zone coalescing behind the tool to form a solid-phase joint as the tool moves forward [11].
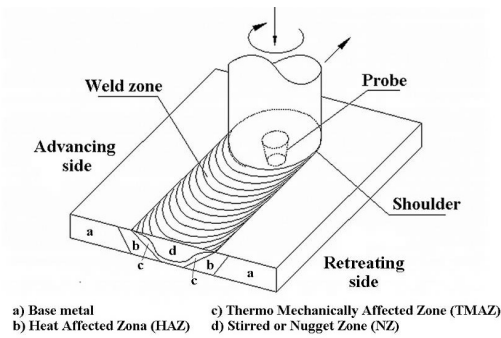
Fig. 1. A schematic illustration of FSW butt-joint. The two sheets have been represented transparent to show the probe. Typical FSW terminology is also indicated.

Although FSW is a solid-state joining process, which produces low-distortion welds, significant levels of residual stress can be present in the weld and they can exert a significant effect on the post-weld mechanical properties, particularly the fatigue ones [12-14]. Since fatigue is the primary cause of engineering failures, fatigue performance of an FSW joint is one of the most important properties to estimate the failure behaviour of friction stir welded structures.

It is clear that the FSW tool is a crucial part of the process; its design is the key to the successful application of the process to a great range of materials and over a wide range of thicknesses [15]. This is why many researchers have examined the effect of the main features of the tool closely. While the open literature offers several examples of studies on the effect of the probe geometry [16-24], recently supported by finite element analysis (FEA) [22-24], few studies have been published on the effects of the tool shoulder geometry on the joint quality. Only Dawes and Thomas [19] analysed advantages and disadvantages of the scroll shoulder concept, by highlighting some of the tool designs under investigation at the Welding Institute (TWI). The shoulder participates in the process in several ways. The more important contributions are to apply a confining pressure to the plasticized material and to maintain an adequate level of heat in the material, providing for sufficient mixing to occur. Additionally, the shoulder confines displacement material to the weld area and it smoothes out the surface of weld, contributing to a favourable cosmetic appearance [25]. Furthermore, the FSW process leaves circular arcs on the surface due to tool shoulder rotation and translation, which generally act as crack initiation sites in as-welded speci- mens [26, 27]. This is why it is thought that a
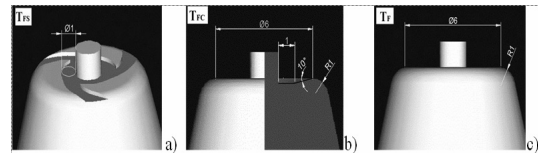

Fig. 2. Tools used and their main dimensions in mm: (a) fillet + scroll tool (T_{FS}); (b) fillet + cavity tool (T_{FC}); (c) fillet tool (T_F).

careful design of the FSW shoulder can improve weld fatigue life.

The present study investigates the influence of three shoulder geometries on the FS joint performance by evaluating, in particular, residual stresses and fatigue life of FSW joints on 1.5 mm thick AA 6082-T6 sheets in butt-joint configuration.

2. Experimental procedure

To carry out the FSW process, two 1.5x125x250 mm AA 6082-T6 sheets were welded for a length of 250 mm parallel to the rolling direction. The 6082 alloy is an Al-Mg-Si alloy containing manganese to increase ductility and toughness. This is an alloy with a composition of 0.95% Si, 0.39% Fe, 0.08% Cu, 0.48% Mn, 0.78% Mg, 0.04% Zn, 0.05% Ti, 0.03% Cr. The T6 condition was obtained through artificial ageing at a temperature of 170-200°C.

The welding process was carried out by rotating the tool at 1810 rpm and at a feed rate of 460 mm/min, with a 2° tilt angle and a 0.1 mm plunge depth.

The tools used were constructed from a 56NiCrMoV7-KU material and they had a cylindrical non-threaded probe with a 1.7 mm diameter and 1.2 mm height. The welds were obtained with three different shoulder geometries; these are the best among those analyzed by the authors in a previous work [28]. All shoulders were characterized by the presence of a fillet on the exterior diameter to reduce the notch produced by the forging effect of the shoulder on the weld face. The three studied shoulders are: a shoulder with a scroll (T_{FS}), a shoulder with a shallow cavity (T_{FC}), and a flat shoulder (T_F) (Fig. 2).

The scroll shoulder was developed at TWI [19]. In this work a modified scroll was adopted, the small shoulder size does not allow the same geometry developed at TWI to be adopted. The scroll track fence was stopped short of the probe (Fig. 2(a)) and the material that enters the gap between the fence and the probe forms a compressed annular ring around the

probe. The used scroll could be considered a hybrid between the scroll and scoop shoulder developed at TWI [19]. A shoulder with shallow cavity was used in numerous previous works and applications [25, 29-31]; the cavity is needed for producing a compressed annular ring of workpiece material around the probe and to prevent the removal of plasticized material.

Visual inspection of roots and faces of the obtained welds was undertaken in order to evaluate the shoulder influence on the joint quality. Furthermore, the bend test (according to UNI 7453-75), supported by penetrant dye to observe also micro-cracks, was carried out on the two sides of the welds. This test has the ability to concentrate the strain in localized region, like the weld, and it is used as a qualitative analysis to detect any cracking in the specimens.

All the joints were cross-sectioned perpendicularly to the welding direction for metallographic analysis. The cross-sections of the metallographic specimens were prepared by standard metallographic techniques.

The Vickers microhardness of the weld zone was measured along a distance of 0.75 mm from the root face on a cross-sectioned specimen in perpendicular to the welding direction with 100 gf load for 15 s.

Transverse tensile tests at room temperature were performed in order to evaluate the mechanical properties of the joints. Four replications were carried out to maintain measurement accuracy. A tensile test was carried out with an initial strain rate of 10^{-4} (mm/mm)*s^{-1}. To determine the tensile strength of the stirred zone, small tensile test specimens were produced. It was checked on the base metal that the tensile curves of the small samples matched with that of standard macroscopic samples, and the resulting precision of the yield stress and ultimate tensile strength (UTS) measurements was estimated as ±5% (Table 1). The tensile tests were carried out on an INSTROM Mod. 4485. Fig. 3(a) shows schematic and main dimensions of longitudinal and transverse tensile tests specimens.

Fatigue tests were also performed by means of the resonant machine RUMUL-50kN on dogbone 10mm width transversal joints; the load ratio was R= $\sigma_{min}/\sigma_{max} = 0.1$. In this way, compressive buckling effects were avoided. A minimum number of 8 specimens for each shoulder geometry were tested and the fatigue curves were obtained. A special gripping tool was designed and attached to the resonant fatigue machine RUMUL to high frequency dynamic testing, allowing good alignment and mounting stiffness to be

Table 1. Comparison between the small tensile test specimen dimension and the standard tensile test specimen on the base metal.

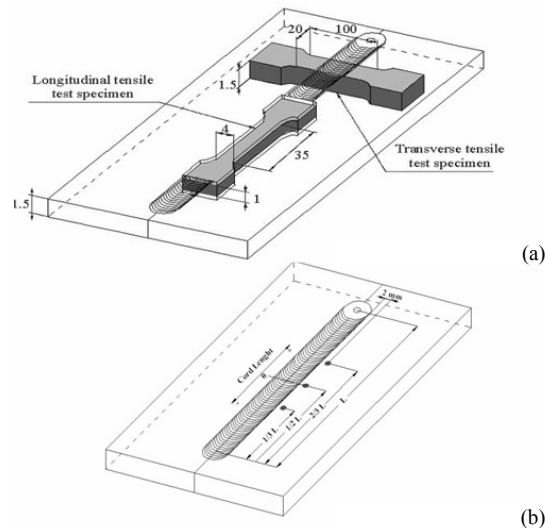|	Yield strength (MPa)	UTS (MPa)	Elongation at break (%)
Standard tensile test specimen	296	331	14
Small tensile test specimen	283	324.8	12.2
Resulting precision	4.4%	1.9%	12.8%

(a)

(b)

Fig. 3. a) Longitudinal and transverse tensile tests specimens. The dimensions are in mm; b) Location of the residual stress measurement points.

achieved.

Finally, the residual stress measurements were performed, by means of the hole-drilling method, according to ASTM E837-01 standards, on all the plates welded with different tool geometries; three measurement points were considered along the weld axis in proximity of the weld toe (Fig. 3(b)). RESTAN automatic system and rectangular rosettes CEA-062UM-120 were used in the half-bridge configuration to compensate for the possible thermal strain. An incremental through hole was drilled by using an advancing speed of 0.08 mm/min with parabolic steps distribution. To obtain correct measurements, the joints, significantly deformed by FSW process, were clamped to the worktable. This operation produced secondary bending strains, which were measured before the hole execution and then elaborated according to the thin shell theory, in order to calculate spuri-

ous bending stress and to correct the real stress relaxed by drilling. The measurement points were chosen at a position equal to 1/3, 1/2 and 2/3 of the weld length, 2 mm away from the weld toe (Fig. 3(b)). The stresses were calculated by means of the power series method in order to consider the non-uniformity of the strains in the thickness.

3. Results and discussion

In the present study, AA 6082-T6 sheets were successfully joined by FSW technique using three different shoulder geometries. The obtained joints showed no porosity or other defects in both top and root weld surfaces in the three welding conditions.

Fig. 4 shows the influence of the shoulder geometries on the top weld surface.
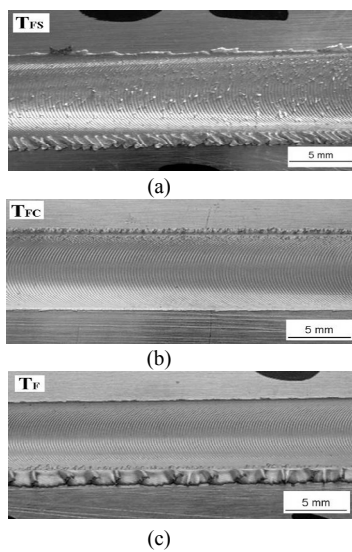

(a)

(b)

(c)

Fig. 4. Top weld surface obtained by the studied tools: (a) fillet + scroll tool; (b) fillet + cavity tool; (c) fillet tool.
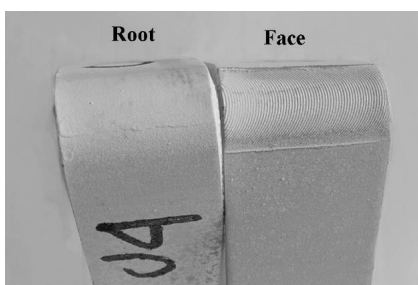

Fig. 5. A typical bend test sample (fillet + cavity tool) showing no cracks for root and face. The penetrant dye was used to support this test.

The T_{FS} tool produced a small amount of flash, but the crown is not smooth. The bead obtained by the T_{FC} tool is characterized by a smooth surface and very little flashes, even if a greater amount of flash is produced during the process, it is removed as a continuous chip. About the T_F, tool smooth crowns and little flashes are produced.

A bend test was carried out on the two sides of the welds to discover defects like root flaws and kissing bond. Furthermore, this test is an important tool to understand about the ductility and toughness of the welds. The three produced welds passed this test. Fig. 5 shows, for example, the bend test carried out on face and root of the T_{FC} specimen.

Fig. 6(a) shows the macrograph of the joint produced with T_{FC} tool. This macrograph does not show any ellipsoidal macrostructural features (the typical FSW onion ring); this is due to the high spindle speed [32] and to non-threaded probe.

FSW gives rise to noticeable microstructure changes. The transverse macro-section reveals the characteristic features of FSW in Al alloys. The joint region is divided into a thermo-mechanically affected zone (TMAZ), and heat affected zone (HAZ). The part of the TMAZ, that experiences high strain and undergoes recrystallization, is known as nugget or stirred zone (NZ); this is the most prominent feature of the friction stir welded zone.

The nugget is approximately symmetric about the weld centerline and it is typically similar in diameter to the probe. The high temperature and the severe plastic deformation during the welding in the stirred zone result in a new equiaxed fine grain structure (Fig. 6(b)) [33], with an estimated grain dimension <4 μm, much smaller and equiaxed when compared to the parent metal microstructure (Fig. 6(d)).

A light influence of shoulder geometry was observed on the nugget grain dimensions due to the different heat power generated by the adopted shoulders. A higher heat input causes a higher peak temperature in the process thermal cycle, which leads to a generation of coarse recrystallized grains [34, 35]. At fixed process parameters (plunge depth, tilt angle, spindle speed, and feed rate), the heat power depends particularly on:

• the contact surface between tool and sheets;
• the material flow under the tool;
• the shoulder pressure on the workpiece.

In the actual experimentation, the T_F shoulder produced the coarsest recrystallized grains. The grain

Table 2. Effect of shoulder geometry on nugget grain dimensions.

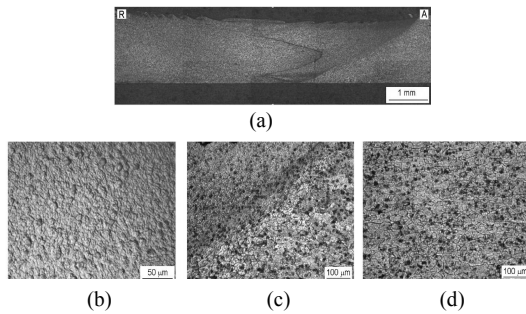| Shoulder geometry	Average grain size (μm)	Std. Dev. (μm)
T_{FS}	3.5	0.5
T_{FC}	2.8	0.3
T_F	3.9	0.4

(a)

(b)　　　　(c)　　　　(d)

Fig. 6. Macrograph and micrographs of weld obtained by fillet + cavity tool: (a) macrograph; (b) stirred zone; (c) TMAZ and HAZ; (d) parent metal. "R" means retreating side, "A" advancing side.
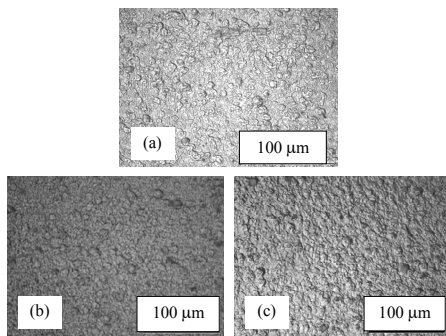

Fig. 7. Micrographs of the grain structures originated by TF (a), TFS (b) and TFC (c) shoulder.

size is reported in Table 2 and the grain structure corresponding to each tool geometry is shown in Fig. 7.

By moving towards the base metal (BM), adjacent to the stirred zone, there is the TMAZ (Fig. 6(c)). This is a transition zone, which corresponds approximately to the edge of the probe. In the TMAZ the tool action resulted in severe bending of grain structure, the parent metal elongated grains were deformed in a flowing patter around the NZ. Although the TMAZ underwent plastic deformation, recrystallization did not occur due to relatively low temperature and no adequate deformations.

Beyond the TMAZ there is the HAZ (Fig. 6(c)),
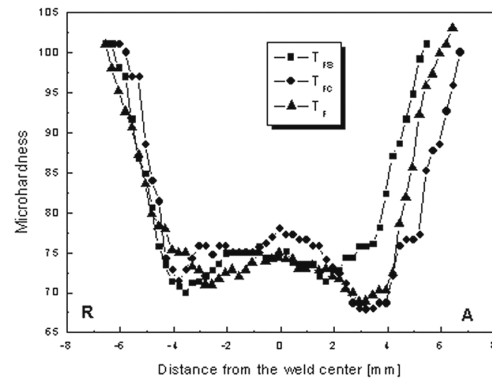
Fig. 8. Horizontal hardness ($HV_{0.1}$) profile across friction stir welds, "A" means advancing side, "R" retreating side.

where the grain size is similar to the BM. This zone experienced a thermal cycle (a peak temperature between 250 and 350°C [36]), but it did not undergo any plastic deformation. Adjacent to the HAZ there is the BM (Fig. 6(d)). The transitions from the TMAZ to the HAZ and from the HAZ to the BM are gradual and not distinguished by any abrupt change in microstructure.

Fig. 8 shows the measured microhardness for the produced welds. FSW created a softened region around the weld center with a significant drop-off of microhardness from the precipitation hardened BM (100-105 $HV_{0.1}$) into the TMAZ/HAZ region (60-70 $HV_{0.1}$).

Svensson [37] shows that in the 6082-T6 the precipitate mainly responsible for hardening (β"-Mg5Si6) is dissolved in both the stirred zone and HAZ. During cooling, precipitation of less hardening particles like β'–Mg1.7Si takes place in the HAZ, but not in the stirred zone. The precipitation of β'–Mg1.7Si in the HAZ is favored by the presence of dispersoids, which act as nucleation sites for precipitates. The peak temperature of the HAZ is about 300 °C; thus the transformation from β"-Mg5Si6 to β'–Mg1.7Si takes place easily, by the dissolution of one phase and the precipitation of the next one. In the stirred zone, the peak temperature is much higher and all Mg-Si precipitates go into solution. From the peak of temperature in the stirred zone, the cooling rate is so high that, even with the presence of dispersoid nucleation sites, this precipitation does not take place [38]. A hardness increase was observed in the stirred zone due to the recrystallization of a very fine grain structure according to the well-known Hall-Patch relationship [39].

A light influence of shoulder geometry was observed on the microhardness. In fact, the contact surface S between tool and sheets resulted in the relation: $S_{TF} > S_{TFS} > S_{TFC}$, which is the reason for which a different thermal input is associated with the three shoulders. Since the grain size is directly related to the thermal input, the micro-hardness results lower in the case of T_F shoulder because of larger grains originated.

Table 3 shows the mechanical properties in transverse direction of the obtained joints; these explain very good properties of yielding, UTS, and ductility which were in good agreement with those reported by Lloyd's Register (LR) [6]. The three specimens showed about the 77% of the UTS of the BM (331 MPa). The fracture position in the welds reflects the position of minimum hardness, which means that the strength of the joints is only function of microhardness distribution and the joints can be considered defect free. Furthermore, during the transverse tensile tests of the welded specimens, the plastic deformation was mainly restricted to the hardness valley; consequently, the low plastic strain at failure value of the standardized test was due to this localization of plastic deformation [40, 41].

The mechanical properties of the stirred zones in the longitudinal direction are summarized in Table 4. When compared to Table 3 the mechanical properties of the material increased in longitudinal direction due to more uniform and finer grain structure (see Fig. 6). The increment in the tensile properties in longitudinal direction was due essentially to the fact that the specimens tested in the longitudinal direction were obtained from the nugget zone. On the contrary, the transversal joints contained the critical section represented by the interface TMAZ/HAZ, which was the weakest region and the principal crack nucleation site. The higher tensile strength of the BM is due to the T6 heat treatment, while the higher elongation of the

stirred zone was due to the very fine grain. The low elongation of the T_F stirred zone was due to micro-defects, which reduced the plastic field of the stirred material. Fig. 9 shows the tensile curves obtained on the base material and on the three types of joints.

The fatigue tests, carried out on the three different series of specimens, revealed some differences in the joints performance. Fig. 10 reports the fatigue curves for the three series of joints.

It can be observed that the joints obtained with fillet + scroll tool (T_{Fs}) shoulder show a worse fatigue behavior and a fatigue limit much lower respect to the remaining type of joints. This result can be explained considering that the T_{Fs} shoulder produced a crown less smooth than that produced by T_F and T_{Fc} shoulders (Fig. 4). The surface irregularities act as sites of crack nucleation and then the joints result poorly resistant to fatigue load. The greater slope of the curve relative to T_{Fs} joints confirms this hypothesis; the slope in fact is an index of the notch sensitivity of the specimens. On the contrary, the joints produced with T_F and T_{Fc} geometries show excellent fatigue behav-
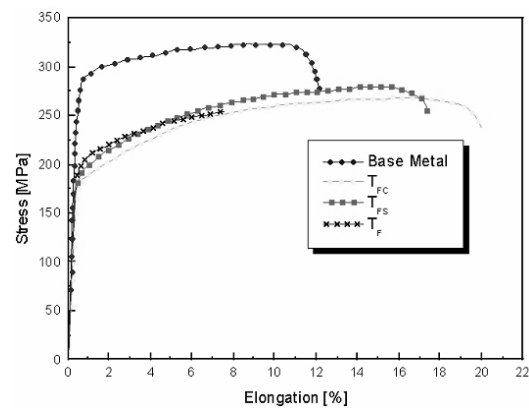

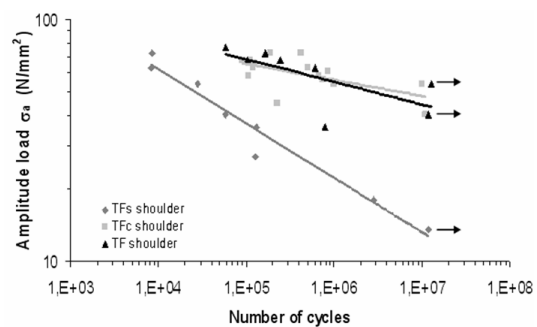Fig. 9. Tensile curves on the base material and welded joints.

Fig. 10. Fatigue curves obtained on the three series of joints.

Table 3: Transverse tensile test: mechanical properties of the studied joints.

	Yield strength (MPa)	UTS (MPa)	Elongation (%)	UTS_W/UTS_{BM}
Base Metal	296	331	14	100%
T_{FS}	155	252	6.8	76%
T_{FC}	152	254	6.5	77%
T_F	156	252	6.2	76%

Table 4. Mechanical properties of the base metal and of the stirred zone tested with micro-specimens.

	Yield strength (MPa)	UTS (MPa)	Elongation (%)	UTS_W/UTS_{BM}
Base Material	283	324.8	12.2	100%
T_{Fs}	193	281.5	17.5	87%
T_{Fc}	181	270	20.1	83%
T_F	194	256	7.9	79%
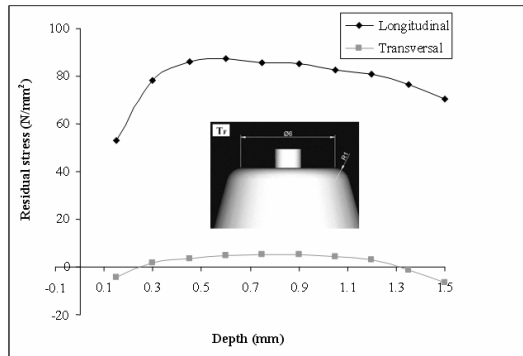
Fig. 11. Residual stress through thickness obtained with T_F shoulder type.

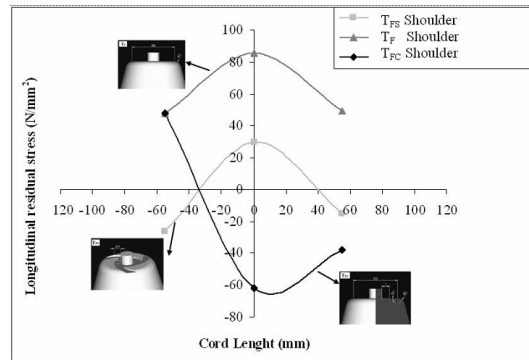Fig. 12. Longitudinal residual stress vs. the weld length at 0.75mm depth.

Fig. 13. Transversal residual stress vs. the weld length at 0.75 mm depth.

ior: the fatigue limit is only reduced of 15-20% with respect to the base material according to previous works [42-44].

Fig. 11 reports an example of residual stress distribution in the thickness; it refers to the measure executed on the T_F joint at middle point of the weld length.

The longitudinal and transversal residual stresses, in correspondence to the half depth vs. the weld length, are reported respectively in Figs. 12 and 13 for the three shoulder typologies.

The longitudinal residual stress results higher than transversal, as in the conventional welded joints. Longitudinal stress distribution was similar for the joints obtained with T_{FS} and T_F shoulder, but the curves relative to different shoulders were shifted. T_F shoulder was associated with maximum longitudinal residual stress that was localized in correspondence to the half-length of the cord. This behavior is justified considering the different heat power generated by the adopted shoulders.

At fixed process parameters (plunge depth, tilt an
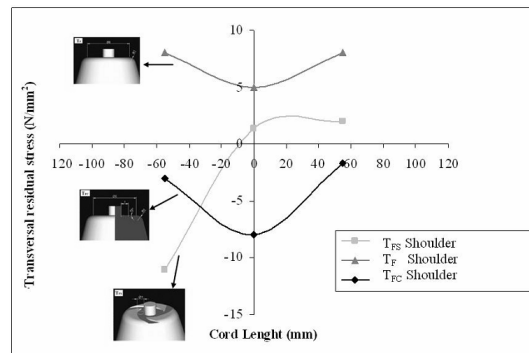
gle, spindle speed, and feed rate), the heat power depends on contact surface between tool and sheets, on the material flow under the tool, and on shoulder pressure on the workpiece. A higher heat input causes a higher peak temperature in the thermal cycle, which produces a higher residual stress field. The larger contact area involved in the FSW process using T_F shoulder originated in a higher thermal input; however, the smaller contact area between the T_{FS} shoulder and material surface originated in a slighter thermal cycle. The low heat generation due to the T_{FS} shoulder produced a generalized low longitudinal residual stress field. The transversal residual stress was low, since it varied in the range of -10 MPa and +10 MPa. In the case of the T_{FC}, the distribution differs from the others; in fact it is very particular.

4. Conclusions

In this work, FSW joints were analyzed in order to

evaluate the influence of three shoulder geometries on the weld performance. At first, the produced joints were characterized by a microstructural and a macroscopic analysis.

A light influence was observed on the nugget grain dimensions due to the different heat input produced by the studied shoulders. The TF shoulder produced the coarsest recrystallized grains because of the higher peak temperature reached in the thermal cycle. The microhardness values in the NZ were coherent with the grain size; the highest value of nugget microhardness was due to a finest structure.

Moreover, shoulder geometries resulted in having an influence on the top weld surface. The T_{FS} tool produced a small amount of flash, but the crown was not smooth. The bead obtained by the T_{FC} tool was characterized by a smooth surface and very little flash. About the T_F one, smooth crowns and little flashes were produced.

Transverse tensile static tests showed that the three specimens presented about 77% of the UTS base material, without differences in the mechanical properties due to shoulder geometry. On the contrary, fatigue tests revealed that the joints obtained with T_{FS} shoulder showed a worse fatigue behavior and a fatigue limit much lower with respect to the remaining types of joints. The joints produced with T_F and T_{FC} geometries showed excellent fatigue behavior with a fatigue limit reduction of about 15-20% respect to the base material.

Finally, residual stress measurements provided longitudinal stress distribution similar for the joints obtained with T_{FS} and T_F shoulder. The curves relative to these shoulders were shifted because of the different heat input produced by the two shoulders. In particular, the residual stress peak value was reduced to about 30 % in the T_{FS} joint. On the contrary, T_{FC} tool showed a very different and particular residual stress distribution.

A relationship between residual stress field and fatigue resistance did not result clear because of very low transversal residual stress level.

Acknowledgment

References

[1] C. D. Mariora, S. J. Andersen, J. Jansen and H. W. Zandberg, The influence of temperature and storage time at RT on nucleation of the β" phase in a 6082 Al-Mg-Si alloy, *Acta Materialia* 51 (2003) 789-796.

[2] L. P. Troeger and E. A. Starke Jr, Microstructural and mechanical characterization of a superplastic 6xxx aluminum alloy, *Material Science and Engineering A* 277 (2000) 102-113.

[3] I. Polmear, *Light Alloys*, Butterwoth-Heinemann, Fourth edition 2006.

[4] M. Ericsson and R. Sandström, Influence of welding speed on the fatigue of friction stir welds, and comparison with MIG and TIG, *International Journal of Fatigue* 25 (2003) 1379-1387.

[5] S. J. Maddox, Review of fatigue assessment procedures for welded aluminium structures, *International Journal of Fatigue* 25 (2003) 1359-1378.

[6] J. Przydatek, A ship classification view on friction stir welding, in: Proc. of 1st *International Friction Stir Welding Symp.*, CA, USA, 14-16 Jun., 1999

[7] J. Mononen, M. Sirén and H. Hänninen, Cost comparison of FSW and MIG welded Aluminium panels, Proc. of the 3rd *International Friction Stir Welding Symp.*, Kobe, Japan, 27-28 September 2001.

[8] W. M. Thomas, E. D. Nicholas, J. C. Needham, M. G. Murch, P. Templesmith and C. J. Dawes, International Patent Application No. PCT/GB92/02203.

[9] J.-Q. Su, T. W. Nelson, R. Mishra and M. Mahoney, Microstructural investigation of friction stir welded 7050-T651 aluminium, *Acta Materialia* 51 (2003) 713-729.

[10] P. Cavaliere, E. CerriI and A. Squillace, Mechanical response of 2024-7075 aluminium alloys joined by Friction Stir Welding, *Journal of Materials Science* 40 (2005) 3669-3676.

[11] W. M. Thomas, E. D. Nicholas and M. Gittos, Friction based technology for aluminium, Proc. of the *Aluminium 98 Conference*, Essen, Germany, 23-24 September 1998.

[12] M. B. Prime, T. Gnäupel-Herold, J. A. Baumann, R. J. Lederich, D. M .Bowden and R. J. Sebring, Residual stress measurement in a thick, dissimilar aluminum alloy friction stir weld, *Acta Materialia* 54 (2006) 4013 – 4021.

[13] R. John, K. V. Jata and K. Sadananda, Residual stress effects on near-threshold fatigue crack growth in friction stir welds in aerospace alloys, *Interna-*

tional Journal of Fatigue, 25 (2003) 939-948.

[14] L. Fratini and B. Zuccarello, An analysis of through-thickness residual stresses in aluminium FSW butt joints, *International Journal of Machine Tools & Manufacture* 46 (2006) 611-619.

[15] W. M. Thomas, E. D. Nicholas and S. D. Smith, Friction stir welding - tool developments, Paper presented at the Aluminum Joining Symposium during the 2001 *TMS Annual Meeting*, 11-15 February 2001, New Orleans, Louisiana, USA.

[16] M. Boz and A. Kurt, The influence of stirrer geometry on bonding and mechanical properties in friction stir welding process, *Material and Design*, 26 (2004) 343-347.

[17] Barcellona, G. Buffa and L. Fratini, Pin shape effect on friction stir welding of AA 6082-T6 sheets, in: Proc. of 4th CIRP International Seminar on Intelligent Computation in *Manufacturing Engineering (ICME 04)*, Italy, 30 Jun.–2 Jul., 2004, 499-502.

[18] O. T. Midling and G. Rørvik, Effect of tool shoulder material on heat input during friction stir welding, in: Proc. of 1st *International Friction Stir Welding Symp*. Oaks, CA, USA, 14-16 Jun., 1999.

[19] C. J. Dawes and W. M. Thomas, Development of improved tool designs for friction stir welding of aluminium, in: Proc. of 1st *International Friction Stir Welding Symp*. Oaks, CA, USA, 14-16 Jun., 1999.

[20] W. M. Thomas, A. B. M. Braithwaite and R. John, Skew-StirTM Technology, in: Proc. of 3rd *International Friction Stir Welding Symp*. Kobe, Japan, 27-28 Sept., 2001.

[21] H. Fujii, L. Cui, M. Maeda and K. Nogi, Effect of tool shape on mechanical properties and microstructure of friction stir welded aluminum alloys, *Materials Science and Engineering A* 419 (2006) 25-31.

[22] P. A. Cologrove, H. R. Shercliff and P. L. Threadgill, Modelling and development of the TrivexTM friction stir welding tool, in: Proc. of 4th *International Friction Stir Welding Symp*. Utah, USA, 14-16 May, 2003.

[23] P. A. Colegrove and H. R. Shercliff, 3-Dimensional CFD modelling of flow round a threaded friction stir welding tool profile, *Journal of Material Processing Technology* 169 (2005) 320-327.

[24] G. Buffa, J. Hua, R. Shivpuri and L. Fratini, Design of the friction stir welding tool using the continuum based FEM model, *Materials Science and Engineering A* 419 (2006) 381-388.

[25] R. J. Heideman, J. W. T. Scott, C. B. Smith, T. M. Thessin, B. N. Ranganathan, D. F. Bishofberger, Friction Stir Welding Tool, International Patent Application N° PCT/US99/10672, Publication Number WO 99/58288, November 1999.

[26] S. Lomolino, R. Tovo and J. Dos Santos, On the fatigue behaviour and design curves of friction stir butt-welded Al alloys, *International Journal of Fatigue*, 27 (2005) 305-316.

[27] M. N. James, D. G. Hattingh and G. R. Bradley, Weld tool travel speed effects on fatigue life of friction stir welds in 5083 aluminium, *International Journal of Fatigue*, 25 (2003) 1389-1398.

[28] L. A. C. De Filippis, A. D. Ludovico, A. Scialpi and R. Surace, Effect of shoulder geometry in Friction Stir Welding thin sheet of AA 6082 T6, in: Proc. of VII *AITEM International Congress*.

[29] K. Colligan, Dynamic material deformation during friction stir welding of aluminum, in: Proc. of 1st *International Friction Stir Welding Symp*. Oaks, CA, USA, 14-16 Jun., 1999.

[30] M. J. Brooker, A. J. M. van Deudekom, S. W. Kallee and P. D. Sketchley, Applying friction stir welding to the Arianne 5 main motor thrust frame, in: Proc. of 2nd *International Friction Stir Welding Symp*. Sweden, 26-28 Jun., 2000

[31] D. G., Kinchen, Z. Li and G. P. Adams, Mechanical properties of friction stir welds in Al-Li 2195-T8, in: Proc. of the 1st *International Friction Stir Welding Symp*. Oaks, CA, USA, 14-16 Jun., 1999.

[32] G. Biallas, R. Braun, C. Dalle Donne, G. Stianek and W. A. Kaysser, Mechanical properties and corrosion behaviour of friction stir welded 2024-T3, in: Proc. of 1st *International Friction Stir Welding Symp*. Oaks, CA, USA, 14-16 Jun., 1999.

[33] Kh. A. A. Hassan, A. F. Norman, D. A. Price and P. B. Prangnell, Stability of nugget zone grain structures in high strength Al-alloy friction stir welds during solution treatment, *Acta Materialia* 51 (2003) 1923–1936.

[34] D. C. Hofmann and K. S. Vecchio, Submerged friction stir processing (SFSP): An improved method for creating ultra-fine-grained bulk materials, *Materials Science and Engineering A* 402 (2005) 234–241.

[35] S. Benavides, Y. Li, L. E. Murr, D. Brown and J. C. McClure, Low-temperature friction stir welding of

2024 aluminum, *Scripta Materialia* 41(1999) 809-815.

[36] Genevois, A. Deschamps and A. Denquin, B. Doisneau-Cottignies, Quantitative investigation of precipitation and mechanical behaviour for AA2024 friction stir welds, *Acta Materialia* 53 (2005) 2447-2458.

[37] L. E. Svensson and L. Karlsson, Microstructure, hardness and fracture in Friction Stir Welded AA 6082, in: Proc. of 1st *International Friction Stir Welding Symp.* Oaks, CA, USA, 14-16 Jun., 1999

[38] L. E. Svensson, L. Karlsson, H. Larsson, B. Karlsson, M. Fazzini and J. Karlsson, Microstructure and mechanical properties of friction stir welded aluminium alloys with special reference to AA 5083 and AA 6082, *Science and Technology of Welding and Joining* 2000 vol. 5 No. 5.

[39] Y. S. Sato, M. Urata, H. Kokawa and K. Ikeda, Hall/Petch relationship in friction stir welds of equal channel angular-pressed aluminium alloys, *Materials Science and Engineering A* 354 (2003) 298-305.

[40] A. J. Leonard and S. A. Lockyer, Flaws in friction stir welds, in: Proc. of 4th *International Friction Stir Welding Symp.* Utah, USA, 14-16 May, 2003.

[41] U. A. Mercado, T. Ghidini, C. Dalle Donne and R. Braun, Fatigue and corrosion properties of friction stir welded dissimilar aluminium alloys, Proc. of 5th *International Friction Stir Welding Symp.* Metz, France.

[42] A. Scialpi, M. De Giorgi, L.A.C. De Filippis, R. Nobile and F. W. Panella, Mechanical analysis of ultra-thin friction stir welding joined sheets with dissimilar and similar materials, *Materials & Design*, 29 (2008) 928–936.

[43] P. Cavaliere, R. Nobile and F. W. Panella, A. Squillace 'Mechanical and microstructural behaviour of 2024-7075 aluminium alloy sheets joined by friction stir welding' *International Journal of Machine tools and Manufacture*, 46 (2006) 588-594.

[44] P. Cavaliere, R. Nobile, F. W. Panella 'Dissimilar Friction Stir Welded sheets of 2024 and 7075 aluminium alloys: Tensile Strength and Fatigue Resistance' *ICEFA, International Conference on Engineering Failure analysis*, Portugal, July 2004.

Marta De Giorgi received academic degree and Ph.D. degree in Materials Engineering from Lecce University in 1998 and 2002 respectively. She is currently a Post-Doc researcher at Salento University in Lecce, Italy. Dr. De Giorgi's research interests are in the area of fatigue, residual stress, welded joints and advanced materials. She studies these subjects by experimental and numerical means.

Agostino Scialpi graduated with honour in Mechanical Engineering in 2002 from Technical University of Bari, Italy. He attended a Master on Rapid Prototyping Techniques, is qualified as International Welding Inspector (Basic Level, IWI-B) and is Professional Member of The Welding Institute (grade: Graduate). He obtained a PhD in Environmental Engineering in 2006 from Technical University of Bari.

Francesco Panella received full mechanical engineering degree in 1996 and Ph.D. degree in Materials Engineering from Lecce University in 1999. Actual position: Senior Researcher at University of Lecce-Italy and assistant Professor in: Machine Design. Main Research fields: Fatigue, welding, thermo-elasticity and Image correlation techniques for stress analysis, advanced Materials characterisation

Luigi De Filippis graduated in Mechanics Engineering at Polytechnic of Bari, Italy in 1998, he started his career with the Ph.D. Degree (2001) in Advanced Production Systems at Polytechnic of Bari. His scientific activities concerne: numerical simulation and experimental investigation of laser welding, forming and heat treatment; rapid prototyping and reverse engineering.